Pioneer 10 Observations of the Solar Wind Interaction With Jupiter

J. H. WOLFE, J. D. MIHALOV, H. R. COLLARD, AND D. D. MCKIBBIN

Space Physics Branch, NASA Ames Research Center, Moffett Field, California 94035

L. A. FRANK

Department of Physics and Astronomy, University of Iowa, Iowa City, Iowa 52240

D. S. INTRILIGATOR

Physics Department, University of Southern California, Los Angeles, California 90007

Detailed analysis of the Pioneer 10 plasma analyzer experiment flight data during the Jupiter flyby in late November and early December 1973 has been performed. The observations show that the interaction of Jupiter's magnetic field with the solar wind is similar in many ways to that at earth, but the scale size is over 100 times larger. Jupiter is found to have a detached standing bow shock wave of high Alfvén Mach number. Like the earth, Jupiter has a prominent magnetopause that deflects the magnetosheath plasma and excludes its direct entry into the Jovian magnetosphere. Unlike that of the earth, the sunward hemisphere of Jupiter's outer magnetosphere is found to be highly inflated with thermal plasma and a high-beta region that is highly responsive to changes in solar wind dynamic pressure. Observational arguments are presented that tend to discount a thin disklike magnetosphere and to favor a Jovian magnetosphere, albeit one probably considerably flattened in comparison with the earth's magnetosphere, yet still with reasonable thickness. Results concerning the shock jump conditions, the magnetosheath flow field, and inferred internal magnetospheric plasma are presented.

The Pioneer 10 spacecraft was successfully launched from Cape Kennedy on March 3, 1972, aboard an Atlas-Centaur launch vehicle that incorporated a TE-364-4 solid-propellant third stage. At the time, Pioneer 10 attained the highest injection energy ever achieved, as is attested to by the fact that the spacecraft required only 11 hours to cross the lunar orbit. After a 21-month flight the Pioneer 10 spacecraft arrived at its radius of closest approach at Jupiter at a distance of approximately 2.8 R_J (Jovicentric Jupiter radii) on December 4, 1973.

The principal scientific objectives of Pioneer 10 are to investigate the nature of the interplanetary medium beyond the orbit of Mars, including the asteroid belt, and to make direct in situ observations of the planet Jupiter and its environment. The successful flyby of Jupiter by Pioneer 10 achieved the latter objectives; however, the interplanetary objectives are still being pursued in the present postencounter mission beyond Jupiter. Present estimates are that the Pioneer 10 spacecraft can be utilized for interplanetary observations to a solar radial distance of at least 20 AU.

The Pioneer 10 spacecraft and trajectory details have been reported by *Hall* [1974] and are only briefly summarized here. The Pioneer 10 spacecraft weighs 258 kg, including 33 kg for the 11 on-board experiments. Two additional experiments are performed by using the spacecraft *S* band communications system. The spacecraft is spin-stabilized, having a spin rate of 4.8 rpm. The spacecraft spin axis is parallel to the axis of the 2.74-m-diameter high-gain antenna reflector and is kept pointed toward the earth in order to maximize the communication bit rate. The maximum bit rate used during the Jupiter encounter was 1024 bits/s. Spacecraft spin axis precession maneuvers are required periodically in order to maintain earth pointing and were performed approximately 6 days prior to and 2 days after the Jupiter flyby. During the encounter the earth-pointing spacecraft spin axis was oriented at an angle of approximately 9.2° with respect to the spacecraft-sun line in a direction away from the west limb of the sun. Electrical power for the experiments and spacecraft subsystems is supplied by four radioisotope thermoelectric generators (RTG), since a conventional solar cell array is not practical for the large solar distances involved in the Pioneer 10 mission. The RTG's are located approximately 2.4 m from the center of the spacecraft at the end of two long booms. Inspection of in-flight data indicates that these RTG's have produced negligible interference with any of the Pioneer 10 experiments. During the encounter the spacecraft approached Jupiter in the midmorning sector of the sunlit hemisphere and exited near Jupiter's dawn meridian. For details of the flyby trajectory see the paper by *Hall* [1974].

PLASMA ANALYZER INSTRUMENTATION

The Ames Research Center plasma analyzer experiment on Pioneer 10 consists of dual 90° quadrispherical electrostatic analyzers, multiple charged particle detectors, and attendant electronics. This analyzer system is capable of determining the incident plasma distribution parameters over the energy range of 100–18,000 eV for protons and approximately 1–500 eV for electrons. A central, cross-sectional drawing of the analyzer and detector portions of the experiment is shown in Figure 1. The A detector, or high-resolution quadrispherical analyzer (the inner analyzer system shown in Figure 1), has an analyzer constant of 9 (charged particle acceptance energy per unit charge divided by the analyzer plate potential) with an analyzer plate mean radius of 9 cm and 0.5-cm separation. The high-resolution analyzer is used for ion analysis only and utilizes 26 Bendix type CEM 4012 Channeltrons, operated in the pulse-counting mode, for ion detection. The Channeltron detectors are arranged in a semicircle at the base of the analyzer plates and cover the angular range of ±51° with respect to the entrance aperture normal. The Channeltrons have an angular separation of approximately 3° near the cen-

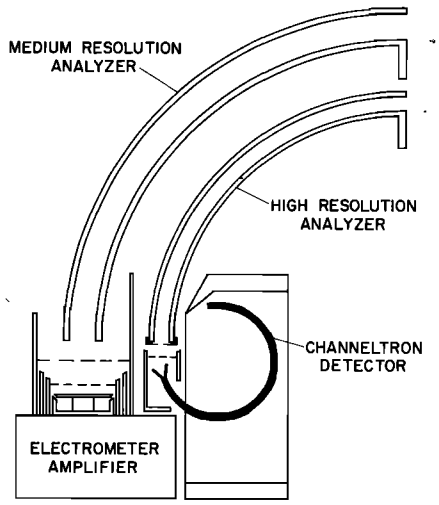

Fig. 1. Central, cross-sectional schematic of the analyzer and detector portions of the Pioneer 10 Ames Research Center plasma analyzer experiment.

tral portion of the analyzer and approximately 8° separation at the extremes of the analyzer. The Channeltron bias voltage can be changed in two sections (left and right halves) by ground command in eight discrete steps over the range of 2600–4400 V. Analysis of flight data has shown that all 26 Channeltrons have operated flawlessly since launch and no appreciable degradation has been observed prior to, during, or subsequent to the Jupiter encounter.

The B detector, or medium-resolution analyzer (the outer analyzer system in Figure 1), has a 12-cm mean radius and 1-cm plate separation, giving an analyzer constant of 6. The medium-resolution analyzer is used for both ion and electron detection and utilizes five flat-surface current collectors and electrometer amplifiers. Each of the three central current collectors has a 15° view width and covers an angular view range of ±22.5° with respect to the entrance aperture normal. The two outside collectors have an angular width of 47.5° each and are located at ±46.25° with respect to the center of the analyzer.

The plasma analyzer experiment is situated on the Pioneer 10 spacecraft such that the entrance apertures view back toward the earth (and therefore the sun) through a wide slit in the back of the spacecraft high-gain antenna reflector. The entrance aperture normals are oriented parallel to the spacecraft spin axis, thus allowing a complete angular scan of the earthward hemisphere every half spacecraft revolution. The edges of the antenna reflector limit instrument viewing to ±73° with respect to the spacecraft spin axis. Although there are a variety of possible operating modes for the experiment, the principal mode utilized during the encounter phase of the Pioneer 10 mission is one in which the energy per unit charge acceptance analyzer potential is stepped every one-half revolution of the spacecraft and all current collectors and Channeltrons are read out at the peak flux roll angle of the spacecraft. Since the medium- and high-resolution analyzers operate independently, a complete cross-check between the two analyzers is possible. The combined analyzer system covers the dynamic range for charged particle fluxes from approximately 1×10^2 to 3×10^9 cm^{-2} s^{-1} and is capable of resolving proton temperatures down to at least 2×10^3 °K. Both analyzers were calibrated prior to launch in the Ames Research Center Plasma Ion Calibration Facility. These prelaunch calibrations are utilized in a least squares fit to the flight data for a variety of possible distribution models in order to determine the plasma ion distribution parameters. Whereas the preliminary report of the Ames Research Center plasma analyzer observations for the Pioneer 10 Jupiter encounter [*Wolfe et al.*, 1974] was based on real time data, the results presented here are based on the analysis of the off-line flight data tapes. An isotropic Maxwellian distribution model has been assumed in the fit to the flight data reported here.

SOLAR WIND–JUPITER INTERACTION

The first unambiguous indication of the interaction of the solar wind with the Jovian magnetic field occurred on November 26, 1973, at approximately 1946 UT spacecraft time. The telemetry signals were actually received at about 2031 UT on earth, ground-received time (GRT), corresponding to a one-way radio propagation time of approximately 45 min. Note that unless it is specifically indicated as GRT, spacecraft time will be used throughout this report. At this time the Pioneer 10 spacecraft was inbound toward Jupiter at a Jovicentric radial distance of 108.9 R_J (R_J = 71,372 km). The two solar wind ion spectra shown in Figure 2 were taken in the interplanetary medium (spectrum on the left) at 1905 UT GRT on November 26, 1973 (day 330), about 1 hour and 25 min before the Jovian bow shock crossing and in the Jovian magnetosheath (spectrum on the right) at 0451 UT GRT on November 27, 1973 (day 331), about 8 hours and 20 min after the shock crossing. Although the ion characteristics in the magnetosheath were quite variable, the spectrum shown in Figure 2 is considered to be typical. The ragged appearance of this spectrum is most likely due to fluctuations in the magnetosheath ion characteristics during the period required to obtain the spectrum and is therefore considered to be an artifact in the data, caused by sample aliasing. The observation of this drastic change in the ion spectral characteristics (Figure 2) is interpreted as the encounter of the Pioneer 10 spacecraft with a detached bow shock wave standing off from Jupiter's magnetosphere and in many respects is quite similar to the case at earth.

For the interplanetary ion spectrum shown in Figure 2 the proton peak is seen near 1 keV, and the doubly charged helium peak near 2 keV. This interplanetary spectrum corresponds to a solar wind convective speed of approximately 441 km s^{-1}, a proton number density of 0.12 cm^{-3}, and an isotropic proton

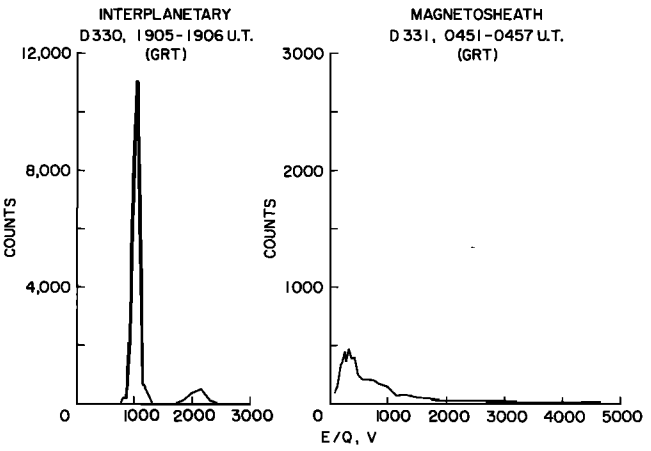

Fig. 2. Comparison of solar wind ion spectra taken upstream and downstream from Jupiter's bow shock for the inbound portion of the Pioneer 10 Jupiter flyby.

temperature of 6.1×10^4 °K. It should be noted that this solar wind speed and number density correspond to an anomalously low solar wind dynamic pressure (by about a factor of 4), compared with that normally observed by this experiment in the interplanetary medium near 5 AU. The ion distribution parameters for this first magnetosheath traversal were mostly obtained from the high-resolution analyzer. The large flow angle (~40°) in the magnetosheath plasma flow direction with respect to the spacecraft spin axis and the high plasma temperature and attendant low density precluded obtaining reliable measurements from the medium-resolution analyzer. This large deflection in flow direction from approximately antisunward to a large angle with respect to the spin axis was observed as the spacecraft crossed the bow shock and with the exception of a 220-min period commencing at approximately 0500 UT on November 27, 1973, persisted throughout the entire magnetosheath traversal. During the above period between 0800 and 0900 UT the flow directions were both toward the center of the plasma analyzer acceptance angle, and in addition, the plasma currents were enhanced. Average magnetosheath plasma distribution parameters of a bulk speed of 273 km s^{-1}, a proton number density of 0.62 cm^{-3}, and a proton temperature of 3.5×10^5 °K were calculated for this time. The distribution parameters for the magnetosheath spectrum of Figure 2 are similar, and here the bulk velocity is approximately 191 km s^{-1}, and the isotropic temperature is approximately 2×10^5 °K. The magnetosheath flow field characteristics are discussed in more detail in the next section.

At 1953 UT on November 27, 1973, the incident plasma ion flux abruptly dropped below the sensitivity threshold for both the high- and the medium-resolution analyzers. At this time the Pioneer 10 spacecraft was located at a Jovicentric radial distance of 96.4 R_J. This termination of the magnetosheath plasma flow is interpreted as the crossing of the magnetopause boundary and penetration into Jupiter's magnetosphere by Pioneer 10 and is presumed to be due to the exclusion and deflection of the magnetosheath plasma by the equal and opposite pressure exerted by Jupiter's outer magnetic field and its internal gas. As was the case for the bow shock, Jupiter's magnetopause also seems in many ways similar to earth's.

As the spacecraft proceeded inbound, magnetosheath plasma, flowing at large angles with respect to the spacecraft spin axis, was again observed at 0233 UT on December 1, 1973, corresponding to a radial distance of 54.3 R_J. The observation of magnetosheath plasma persisted for approximately 11 hours and was again abruptly terminated at 1336 UT on December 1, 1973, at 46.5 R_J. At present there are two apparent explanations for the second magnetopause traversal observed during the inbound portion of the Pioneer 10 trajectory. The first is that the interplanetary solar wind dynamic pressure increased to such an extent that the entire Jovian magnetosphere contracted down to a size such that the spacecraft was again located in the magnetosheath. An alternative possibility is that the topology of Jupiter's magnetosphere is such that a simple change in the interplanetary solar wind flow direction (with little or no change in dynamic pressure) deflected Jupiter's magnetosphere so that the spacecraft was located within the magnetosheath. The present evidence seems strongly to favor the former explanation and is discussed further in the summary section.

During the remainder of the Pioneer 10 traversal of the Jovian magnetosphere, sporadic plasma ion fluxes were observed, but their analysis has been complicated by high background rates due to penetrating energetic electrons and protons. Magnetospheric plasma ion observations are very preliminary at this time and are not reported here. Other than these high background rates observed in Jupiter's inner magnetosphere the plasma analyzer experiment successfully withstood Jupiter's intense radiation zones and recrossed Jupiter's magnetopause on the outbound leg of the trajectory at 1153 UT on December 10, 1973, at a distance of 97.9 R_J. In contrast to the inbound portion of the flyby trajectory, where the bow shock was observed once and the magnetopause was crossed three times, during the outbound leg the magnetopause was crossed five times, and there were 17 positively identifiable shock crossings. All of the shock and magnetopause observations during the Pioneer 10 Jupiter flyby are listed in Table 1 for both the inbound and the outbound passes. Table 1 shows that the last shock crossing occurred at 1928 UT on December 22, 1973, at a distance of 242.6 R_J. Thus the Jupiter encounter for the plasma analyzer experiment lasted nearly a month!

Two further plasma observations associated with Jupiter's bow shock may be noted. A period of approximately 14-min duration that began 13 hours and 43 min after the last bow shock crossing listed in Table 1 exhibits greatly reduced plasma flux and some flow deflection that probably indicates a movement of Jupiter's bow shock near the spacecraft. However, a crossing of the bow shock cannot be positively identified here. In addition, 18 min before the first bow shock crossing the solar wind plasma flux was apparently temporarily greatly reduced; this could be an interplanetary effect rather than an approach of the bow shock near the spacecraft, since a large flow deflection was not observed.

The magnetosheath boundary traversals given in Table 1 are illustrated in Figure 3, which shows the Pioneer 10 Jupiter encounter trajectory projected onto Jupiter's orbital plane. Each shock (S) and magnetopause (M) location is identified along the spacecraft trajectory at the position where it was observed. Note that in the outbound leg the point identifying the second magnetopause location actually represents two closely spaced magnetopause crossings and a burst of plasma that could represent two further crossings and the point identifying the last shock observation represents five separate crossings (Table 1). The dashed lines in Figure 3 are for illustrative purposes only and are meant to show the extremes in magnetopause and shock locations during the Pioneer 10 flyby. The boundary shapes and shock standoff distances have been determined from the gas dynamic analog [*Spreiter et al.*, 1966]. The shock and magnetopause boundaries have arbitrarily been made symmetrical with respect to the Jupiter–solar wind line. The outermost shock and magnetopause boundaries have been scaled to the last shock crossing for the outbound leg. Similarly, the innermost shock and magnetopause boundaries have been scaled to the last magnetopause crossing for the inbound leg.

It is interesting to consider the large scale size of Jupiter's magnetosphere and shock front. For example, the width of the shock front for its largest extent (based on the last shock crossing on the outbound leg and the assumed symmetry and shape illustrated in Figure 3) would correspond to a distance of approximately 485 R_J, as measured across the dawn-dusk meridian. This value is equivalent to a width of 0.23 AU and is more than 2 orders of magnitude larger than the nominal width of the earth's bow shock. The large extent over which Jupiter's magnetosphere can evidently move indicates that it is

TABLE 1. Jupiter Magnetosheath Boundary Locations Observed During the Pioneer 10 Flyby

Spacecraft Location	Boundary Observation	Spacecraft Time		Distance, R_J
		Date, 1973	Hours, UT	
		Inbound		
IP				
	S	Nov. 26	1946 ± 2	108.90
MSH				
	M	Nov. 27	1953 ± 2	96.36
MS				
	M	Dec. 1	0233 ± 6	54.32
MSH				
	M	Dec. 1	1335.7 ± 2.2	46.50
MS				
		Outbound		
MS				
	M	Dec. 10	1153.4 ± 0.5	97.92
MSH				
	M	Dec. 12	0943.2 ± 0.5	121.52
MS				
	M	Dec. 12	0958.2 ± 0.5	121.66
MSH				
	S	Dec. 12	1453.2 ± 1.5	124.14
IP				
	S	Dec. 12	1950.7 ± 6	126.64
MSH				
	M	Dec. 13	0158.1 ± 0.5	129.73
MS				
	M	Dec. 14	1850 ± 1	150.08
MSH				
	S	Dec. 18	0328 ± 1	188.87
IP				
	S	Dec. 20	2145.1 ± 0.5	220.54
MSH				
	S	Dec. 20	2233.9 ± 0.5	221.41
IP				
	S	Dec. 21	0212 ± 2	223.13
MSH				
	S	Dec. 21	0643 ± 2	225.27
IP				
	S	Dec. 21	1027 ± 2.8	227.04
MSH				
	S	Dec. 21	1158 ± 2	227.76
IP				
	S	Dec. 21	1848.5 ± 9.5	230.99
MSH				
	S	Dec. 21	1929.2 ± 2.9	231.31
IP				
	S	Dec. 22	0605 ± 10	236.31
MSH				
	S	Dec. 22	1757.6 ± 1.8	241.44
IP				
	S	Dec. 22	1805 ± 1	241.97
MSH				
	S	Dec. 22	1811.8 ± 1.5	242.02
IP				
	S	Dec. 22	1815.7 ± 0.1	242.05
MSH				
	S	Dec. 22	1928.0 ± 2.7	242.62
IP				

IP, interplanetary medium; MSH, magnetosheath; MS, magnetosphere; S, shock crossing; and M, magnetopause crossing. Note: MS plasma bursts at 0225 and 1345, December 1, and 0947.7, December 12. Greatly reduced MSH plasma flux at 1324.8 ± 0.5, December 1.

extremely responsive to changes in the incident solar wind conditions.

MAGNETOSHEATH FLOW FIELD

Figure 4 gives ½-hour averages of proton bulk velocities, number densities, and isotropic temperatures observed during November 26 and 27, 1973, as Pioneer 10 first crossed Jupiter's bow shock and magnetosheath. The velocities presented do not have the spacecraft velocity subtracted. A correction for this may be estimated by use of the spacecraft velocity components during this 2-day period, which are 7.2–7.5 km s^{-1} in the antisolar direction and 6.7 ± 0.1 km s^{-1} in the direction of planetary motion, parallel to the ecliptic plane.

The bow shock and magnetopause locations as observed by the plasma analyzer are indicated with a solid and an open arrow, respectively, at the bottom of Figure 4. As was stated previously, within the inbound magnetosheath, plasma parameters could not be determined by the medium-resolution detector, except between 0800 and 0900 UT on November 27, when the plasma flux was enhanced while the flow direction was toward the center of the instrument angular acceptance range. For this time period, proton velocities and temperatures

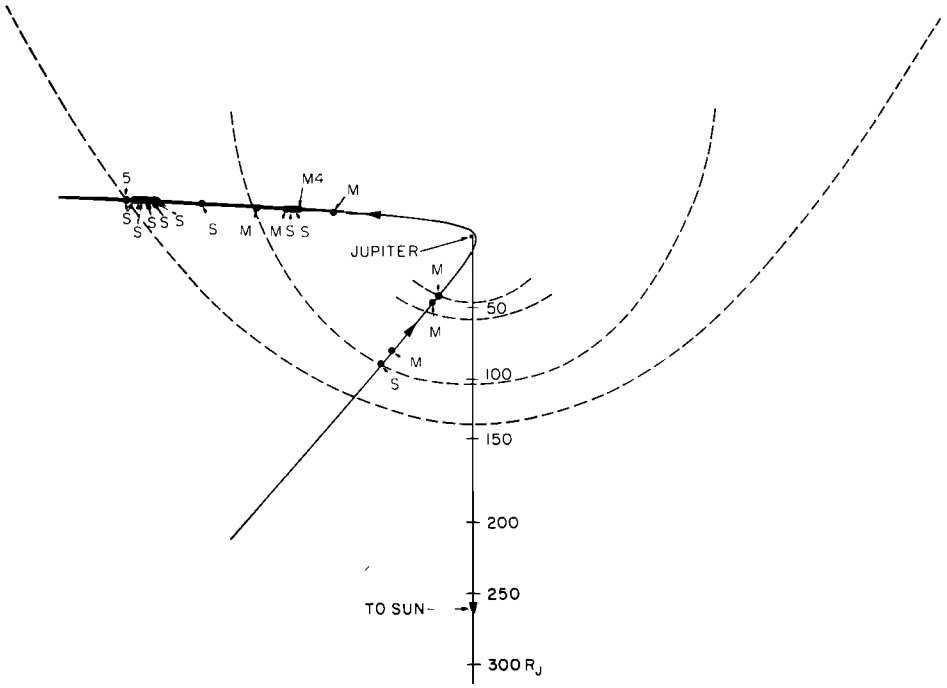

Fig. 3. Locations of the shock (S) and magnetopause (M) crossings on the Pioneer 10 Jupiter flyby trajectory, which has been projected onto Jupiter's orbital plane. The inner and outer pairs of dash lines illustrate the observed extremes of position of the magnetopause and standing bow shock. The shape of the boundaries and the shock standoff distances are based on the gas dynamic analog and are scaled to the actual boundary observations.

from the medium-resolution detector were determined by a fit of a Maxwellian distribution to the data. The average proton number density obtained is 0.62 cm^{-3}. These data have not been included in Figure 4. For all magnetosheath times on the figure, ½-hour averages of proton bulk velocities and isotropic temperatures from the high-resolution detector are given. Owing to the incomplete analysis of the high-resolution detector data, values for the ion densities are not yet available.

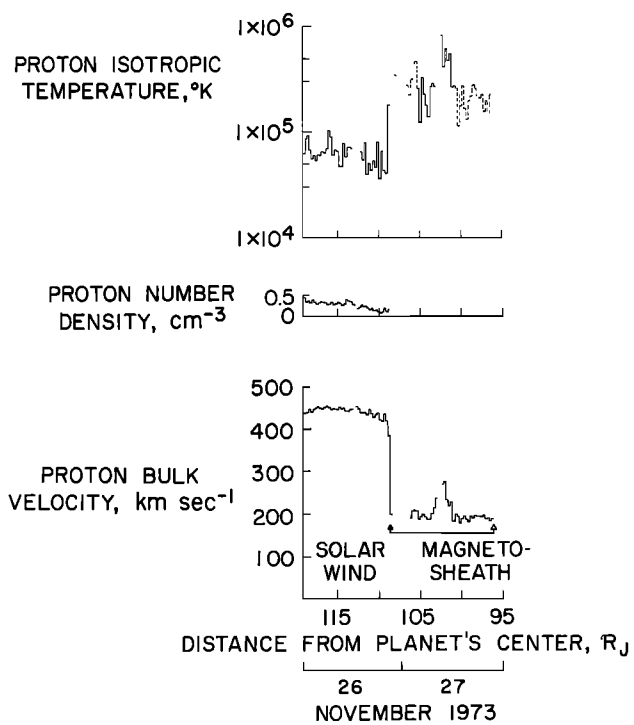

Fig. 4. Half-hour averages of the proton bulk velocities, number densities, and isotropic temperatures observed for November 26 and 27, 1973, corresponding to the first crossing of Jupiter's bow shock and magnetosheath. Temperatures indicated with dashes are approximate values derived from scans through the velocity distribution that do not include the peak.

The plasma parameters from the medium-resolution detector given here are calculated by a linear least squares fit of the flight data to a convecting isotropic temperature Maxwell-Boltzmann distribution by using a representation of the detector response condensed from detailed laboratory calibration data.

The velocities and temperatures from the high-resolution detector data are obtained by following the formalism of a calculation of the moments of the plasma velocity distribution. From 0244 to 1127 UT on November 27, data from the inner Channeltron that scans through the peak of the proton velocity distribution were used to obtain the proton bulk velocities and isotropic temperatures for Figure 4. Similarly, the data from one of the outermost two Channeltrons were used for the remainder of the magnetosheath times on the figure. The proton counts of the inner Channeltrons are integrated for 1/512, 1/128, 1/64, or 1/32 spacecraft revolution, subject to ground command. Similarly, for the outermost Channeltron used here these counts are integrated, except during special instrument modes, for 31/64 of a spacecraft revolution. When data from the outermost Channeltron are used here, it is because the statistics provided by the other Channeltrons are felt to be too poor to provide reliable plasma parameters with their data alone. In these cases the velocities derived from the outermost Channeltron are lower limits, since this Channeltron does not scan through the maximum of the proton velocity distribution. These derived velocity values are then corrected by dividing by cos δ, where δ is the angle between the view direction of the outermost Channeltron and the peak of the velocity distribution as determined from the data of the remaining Channeltrons.

The bulk velocity is obtained from

$$N\langle \mathbf{p} \rangle = mN(\langle \mathbf{V} \rangle - \mathbf{u}) = 0$$

and this condition is approximated by

$$u \sim \frac{\sum (n_i/v_i^3)}{\sum (n_i/v_i^4)}$$

The first equation is written in terms of a velocity value u such that the momentum density of the protons is zero in a reference frame moving with this velocity. In these equations, n_i is the count value for the ith velocity (energy) analyzer acceptance value v_i, m is the proton mass, N is the proton volume density, $\langle \mathbf{p} \rangle$ is the vector average proton momentum, and $\langle \mathbf{V} \rangle - \mathbf{u}$ is the vector average proton velocity (thermal velocity) referred to the proton bulk velocity u. The isotropic temperature value is obtained from

$$T = \frac{m}{k} \frac{\sum (n_i/v_i^4)(u - v_i)^2}{\sum (n_i/v_i^4)}$$

where k is Boltzmann's constant. When these calculations are performed, an attempt is made to eliminate detector responses due to He^{++} by not using the portion of the spectrum for E/q (energy per unit charge) values 2 or more times greater than that for the peak counts. This is one reason why the magnetosheath temperatures from the high-resolution detector are lower limits, since the interplanetary spectra just upstream from the shock indicate a negligibly low He^{++} solar wind abundance at that time (Figure 2). Thus the high-energy portion of a nonthermal distribution would be ignored. Also, the roll integration of the outermost Channeltron count rates introduces an effect that could broaden the velocity distributions used in the temperature calculation. The medium-resolution detector magnetosheath temperatures for 0800 to 0900 UT on November 27 agree with the high-resolution detector temperatures given on Figure 4, presumably because the medium-resolution detector data have been fit to an isotropic Maxwellian distribution, so that the non-Maxwellian portions of the spectrum also tend to be ignored. Consequently, the values for the magnetosheath temperature calculated from the medium-resolution detector data also tend to be lower limits.

The medium-resolution detector magnetosheath proton bulk velocities determined for the 60-min period beginning at 0800 UT on November 27, 1973, were ~25 km s^{-1} lower than the high-resolution detector values. This small velocity difference is presumably due to the difference in sensitivity to the nonthermal part of the velocity distribution in the two methods used for velocity calculation.

Gaps in the data of Figure 4 are sometimes due to ground-commanded changes of instrument status into special modes for which the results are not included here. Some gaps are also caused by brief data losses in the ground data network.

The plasma conditions observed during the second magnetosheath traversal (54.3–46.5 R_J) were somewhat similar to those observed during the first traversal with one important difference. With the exception of the enhanced speed, temperature, and density values observed between approximately 0800 and 1000 UT on November 27 for the first magnetosheath traversal the speed and temperature values observed during the second traversal were comparable. The density, however, was observed to be almost an order of magnitude higher for the second traversal.

The second magnetosheath traversal proton bulk velocities were in the 165 to 210 km s^{-1} range, and the temperature was observed to vary from about 6×10^4 °K to 5×10^5 °K. Both the higher velocities and the higher temperatures were observed near the end of the traversal. The unaberrated polar and azimuthal flow directions at the beginning of the traversal were ~40° southward and ~19° in the direction of planetary motion, respectively. Near ~0715 UT there are several samples with lower limit southward flow directions near 0° and azimuthal flow directions of $\gtrsim 35°$ in the direction of planetary motion. Near the end of the traversal the flow direction is ~15°–25° southward and ~30°–35° in the direction of planetary motion. Thus not only were the densities greater during the second traversal but the flow deflections were also greater than those observed for the first traversal.

Figure 5 gives ½-hour averages of proton bulk velocities, number densities, isotropic temperatures, and hourly averages of unaberrated azimuthal and polar angles for the outbound traversal of Jupiter's magnetosheath by Pioneer 10, during December 10–22, 1973. The flow direction average polar, $\bar{\theta}$ and azimuthal $\bar{\varphi}$ angles are composed from individual samples θ_i and φ_i by using the expressions

$$\sin \bar{\theta} = (\sum \sin \theta_i)[(\sum \cos \theta_i \cos \varphi_i)^2 + (\sum \cos \theta_i \sin \varphi_i)^2 + (\sum \sin \theta_i)^2]^{-1/2}$$

$$\tan \bar{\varphi} = \frac{\sum \cos \theta_i \sin \varphi_i}{\sum \cos \theta_i \cos \varphi_i}$$

In a spacecraft-centered solar ecliptic coordinate system, the polar angles θ are positive for southward flow, whereas azimuthal angles φ are positive for solar wind flow deviated in the direction opposite planetary motion. The velocity averages given on this figure have not had the spacecraft velocity subtracted. The correction for this may be estimated by using the spacecraft velocity components, which are 0.4 and 23.7 km s^{-1} in the antisolar direction and the direction of planetary motion (but parallel to the ecliptic), respectively, at 1200 UT on December 10. These velocity components are 0.7 and 22.7 km s^{-1}, respectively, at 0000 UT on December 22. The times of 17 bow shock and five magnetosheath crossings (Table 1) are shown on Figure 5 and are indicated by open and solid arrows, respectively, at the bottom of the figure.

Gaps in the plots of parameters on Figure 5 are sometimes due to ground-commanded changes into experiment modes for which plasma parameter calculations are not available for inclusion in this paper. In addition, at some times in the magnetosheath the medium-resolution detector currents are reduced to the instrument noise levels, whereas the high-resolution detector data have not been analyzed for this time period. During the times on Figure 5 within the magnetosphere, proton fluxes are not detectable in the data with the standard techniques used for the other portions of the figure.

Inspection of Figure 5 shows large bulk velocity excursions for December 10 and early on December 11. Part of the cause of this may be a response of the computer routine that calculates the plasma parameters to an apparent non-Maxwellian plasma spectrum with a very broad proton maximum. At various times the computer program weights the higher-velocity portion of this broad maximum more or less heavily and thus calculates higher or lower proton bulk velocities.

The magnetopause crossings from 0943 to 0958 UT on December 12 have the characteristic of relatively gradual disappearance or reappearance of all observable plasma flux as the magnetosphere is entered or left behind.

Perhaps the most striking features in Figure 5 are the much less dramatic changes in velocity and density for the shock crossings further away from the planet than for the inbound shock crossing or for closer crossings for the outbound leg. Note, however, that relatively large changes in the proton temperature are always observed regardless of shock location. As is the case at earth, this finding probably indicates that Jupiter's bow shock becomes weaker for greater and greater angles and distances from the subsolar point. For this reason the determinations of the shock locations reported here have relied more heavily on temperature changes than on any other parameter, although the flow direction changes are usually very prominent in the high-resolution detector data.

In addition, as was the case for the inbound magnetosheath traversals, the flow directions in the magnetosheath seen in Figure 5 are greatly deviated, in general agreement with those expected for plasma flow around a relatively blunt magnetosphere. A large southward component in the magnetosheath flow was observed for the inbound leg when the spacecraft was below Jupiter's orbital plane. Here a large northward component in the flow is seen where for the outbound magnetosheath traversal the spacecraft is above Jupiter's orbital plane.

SHOCK JUMP CONDITIONS

Table 2 gives the measured average and calculated best-estimate shock jump parameters and 'sigma noise parameters' for the inbound Jupiter bow shock crossing observed by Pioneer 10. The best-estimate values are calculated by use of the *Lepping and Argentiero* [1970] program without an error cone calculation. The vector components in the table are given in the standard right-handed ecliptic-type coordinate system with positive x in the solar direction and positive z northward. Subscripts 1 and 2 refer to upstream and downstream parameters, respectively; B and n are the magnetic field (E. J. Smith, private communication, 1974) and the proton number density, respectively; and W is the difference between downstream and upstream bulk velocity components. Eight upstream and seven downstream magnetic field 1-min averages were used as well as three upstream and three downstream proton bulk velocity samples and three upstream proton number density samples. Only the first of the three downstream speed values was used. The basic upstream plasma sampling period is 5.4 min. The downstream proton number density best-estimate value is that which produces the best fit when a variety of assumed values are entered into the program as input observed data. The downstream number densities immediately adjacent to the shock are difficult to measure accurately because of the apparent proximity of the flow direction to the outer edges of the detector acceptance.

The measured and calculated best-estimate parameters agree well except for the x component of the downstream magnetic field (B_{2x} in Table 2). The measured values closest to the shock transition are higher and so are closer to although they are still lower than the calculated best-estimate value.

The calculated best-fit shock normal is (0.731, −0.233, −0.641), indicating only an 18° angle between the solar direction and the projection of the shock normal on the plane that contains both the solar direction and the y axis of the coordinate system. A 40° southward tilt of the shock normal is also indicated. The apparent large southward plasma flow deflection behind the shock is suggestive of solar wind interaction with a large blunt obstacle. The calculated best-fit thermal pressure difference across the shock (downstream less upstream) is 2×10^{-10} dyn cm^{-2}. The measured pressure difference due to protons alone is of the order of 13×10^{-12} dyn cm^{-2}, when it is assumed that the downstream proton number density is 0.33 cm^{-3}. The Alfvén Mach number of the shock, when it is assumed to be stationary, is 14. when the best-fit shock orientation is used.

Table 3 gives measured average and calculated best-estimate shock jump parameters, and sigma noise parameters for the third shock crossing observed by Pioneer 10 on the outbound leg. The same techniques are used as those employed for the inbound shock calculations. Seventeen upstream and ten downstream 1-min magnetic field averages (E. J. Smith, private communication, 1974) were used. Two upstream and three downstream proton density measurements were used, taken at 2.8-min intervals. Only one upstream proton bulk velocity sample and one downstream proton bulk velocity sample were used. The vector components in Table 3 are given in the same coordinate system that was used for the inbound case. As was done before, subscripts 1 and 2 refer to upstream and downstream parameters, respectively; B and n are the magnetic field and the proton number density, respectively; and the W_i are the differences between downstream and upstream bulk velocity components.

Here again there is good agreement between measured and best-estimate parameters. The best-fit calculated shock normal (outward) is (0.379, −0.887, 0.264), indicating a 67° angle between the solar direction and the projection of the normal on the plane that contains both the solar direction and the y axis of the coordinate system. This angle appears to be ~15° larger than that expected for a shock shape like that of the earth. A 15° northward tilt of the normal is also indicated. The calculated best-fit thermal pressure difference across the shock is -2×10^{-11} dyn cm^{-2}. The measured pressure difference due to protons alone is 5×10^{-13} dyn cm^{-2}. The Alfvén Mach number of the shock for a shock stationary with respect to Jupiter is 8.5 when the best-fit orientation is used.

MAGNETOSPHERIC PLASMA

Table 4 gives estimates of magnetospheric plasma properties obtained from two different methods. The first method assumes pressure balance across the magnetopause, expressed by

$$n_1 k(T_{e1} + T_{i1}) + \frac{B_1^2}{2\mu_0} = n_2 k(T_{e2} + T_{i2}) + \frac{B_2^2}{2\mu_0}$$

The second method uses the aerodynamic analogy [cf. *Spreiter et al.*, 1966] and is described below. In the above pressure balance equation the subscripts 1 and 2 refer to magnetosheath and magnetosphere parameters, respectively; n is the plasma ion number density; T_e and T_i are the electron and ion temperatures, respectively; B is the magnetic field magnitude; k is Boltzmann's constant; and μ_0 is the magnetic permeability of free space, equal to $4\pi \times 10^{-7}$ H m^{-1}; $T_e \sim T_i$ is assumed, and $T_{i2} \sim 5 \times 10^4$ °K (~4-eV electrons) is assumed on the basis of the measured magnetospheric electron energy spectra.

The magnetosheath values for the December 13 crossing are less reliable than the others owing to divergence of the plasma flow direction near the outer limit of the medium-resolution

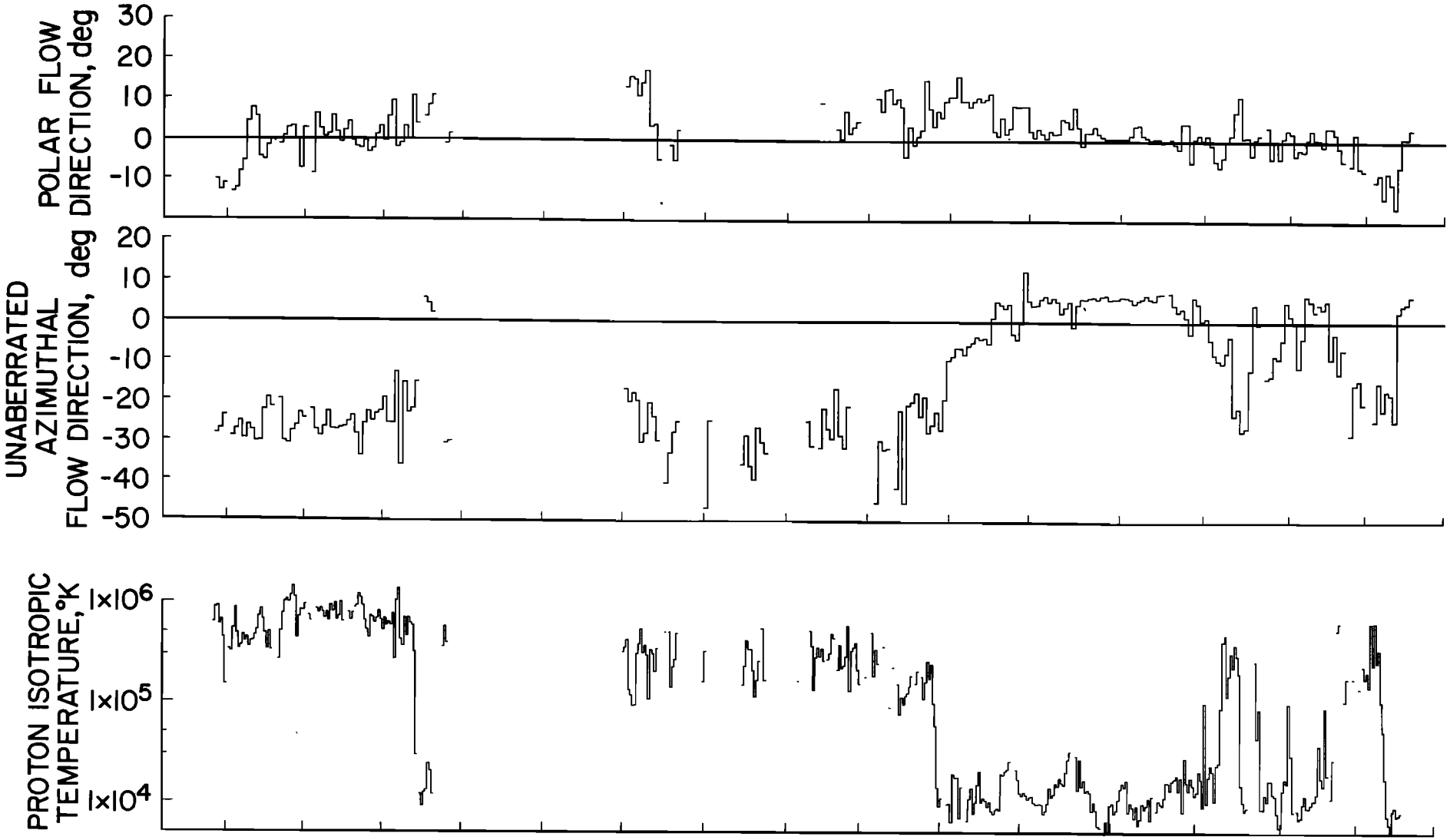
POLAR FLOW DIRECTION, deg
30
20
10
0
-10
UNABERRATED AZIMUTHAL FLOW DIRECTION, deg
20
10
0
-10
-20
-30
-40
-50
PROTON ISOTROPIC TEMPERATURE, °K
1×10^6
1×10^5
1×10^4

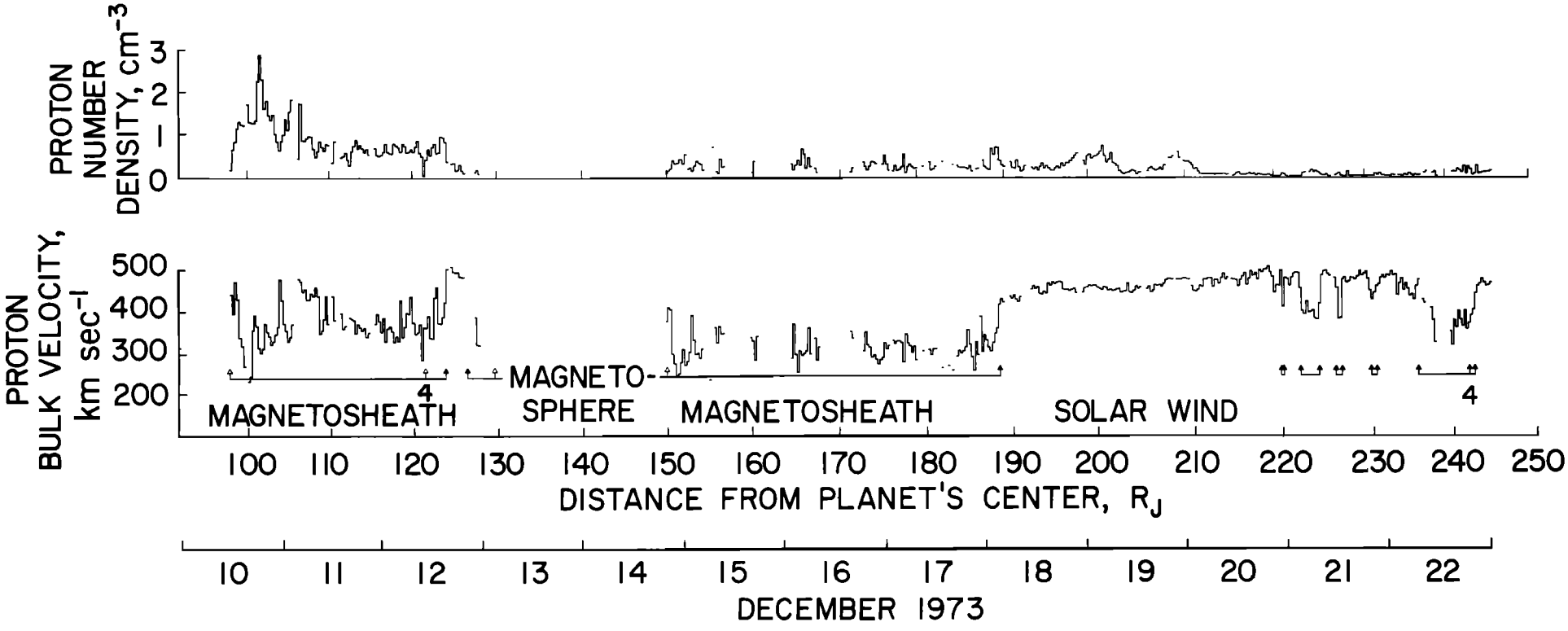

Fig. 5. Half-hour averages of the proton bulk velocities, number densities, isotropic temperatures, and hourly averages of unaberrated azimuthal and polar angles for the outbound traversal of Jupiter's magnetosheath by Pioneer 10 during December 10–22, 1973.

TABLE 2. Measured Average and Calculated Best-Estimate Shock Jump Parameters and Sigma Noise Parameters for the Pioneer 10 Inbound Jupiter Bow Shock Crossing

Parameter*	Average Value	σ	Best-Estimate Value
B_{1x}	-0.46	0.14	-0.37
B_{1y}	0.11	0.24	0.19
B_{1z}	-0.01	0.21	-0.02
B_{2x}	-0.18	0.32	-0.58
B_{2y}	0.38	0.53	0.35
B_{2z}	-0.47	0.30	-0.33
W_x	171.	15.	174.
W_y	-54.	20.	-55.
W_z	-172.	35.	-153.
n_1	0.12	0.02	0.14
n_2			0.33

*Units of measure are gammas for B_{1x} through B_{2z}; kilometers per second for W_x, W_y, and W_z; and cm^{-3} for n_1 and n_2.

detector angular acceptance. The December 10 crossing appeared to occur at a time of extreme conditions, and in addition the observed magnetic field profile across the magnetopause (E. J. Smith, private communication, 1974) appears as if a wide layer were crossed, but fields outside this 'layer' are ignored when the results of Table 4 are calculated.

The results in Table 4 obtained with the aerodynamic analogy use Pioneer 10 free-stream plasma parameters obtained closest in time to the indicated magnetopause crossings. Because of the time delay between the magnetospheric and the free-stream measurements by Pioneer 10 this method is less reliable owing to neglect of possible time variations in the external free-stream conditions. The assumed condition is

$$Kmn_1{}^*v^{*2}\cos^2\theta + n_1{}^*k(T_{e1}{}^* + T_{i1}{}^*) + \frac{B_1{}^{*2}}{2\mu_0} = n_2k(T_{e2} + T_{i2}) + \frac{B_2{}^2}{2\mu_0}$$

where m is the proton mass, v is the bulk velocity, the asterisks denote free-stream quantities, K is taken as unity, and θ is the angle between the magnetopause normal and the free-stream plasma flow direction. Angle θ is obtained from calculations made for the case at earth given by *Spreiter et al.* [1966]. The values of θ were tested against calculated values obtained by using the magnetic field measured across the magnetopause (E. J. Smith, private communication, 1974) and by assuming that the magnetopause is a tangential discontinuity, and the earth analogy values were much larger than the calculated values. This result implies a magnetopause body shape comparatively more blunt than that of the earth.

SUMMARY AND CONCLUSIONS

Of particular interest is an understanding of the topology and dynamics of Jupiter's magnetosphere and its interaction with the solar wind. This understanding, of course, is difficult to achieve in a single flyby. There are, however, several clues in the Pioneer 10 data that shed some light on this problem. It is clear that in many respects Jupiter's standing bow shock, magnetosheath flow field, and magnetopause are similar to those of the earth. Both the shock and the magnetopause at Jupiter are observed to be well-defined boundaries, and like that of the earth, Jupiter's bow shock is a strong shock (high Alfvén Mach number). Jupiter's magnetopause, also like earth's, is a relatively sharp boundary between the planetary field and the magnetosheath flow field wherein it deflects the magnetosheath plasma and excludes it from direct entry into the magnetosphere. Finally, as is the case at earth, the observed shock normals and magnetosheath plasma flow directions observed for Jupiter are consistent with the presenting by Jupiter's magnetosphere of a relatively blunt body to the solar wind for the sunward hemisphere.

It is cautioned, however, that earth analogies may be confused owing to the vastly different scale sizes involved. For example, the extent of Jupiter's bow shock, as inferred from the furthest out observed shock crossing, is almost ¼ AU wide as measured across the dawn-dusk meridian. This value is over 2 orders of magnitude larger than the earth's bow shock measured in the same fashion. It is suspected that if Jupiter's magnetosphere were scaled down to the size of the earth's magnetosphere, corresponding to the geocentric distance to the subsolar point, Jupiter's magnetosphere would be considerably flattened in shape in comparison with the earth's. This is strongly suggested by the manner in which Jupiter's magnetic field lines in the outer magnetosphere are greatly elongated and stretched out from the planet [*Smith et al.*, 1974*a*]. The degree to which Jupiter's magnetosphere is flattened is impossible to estimate from the data of this single flyby, but the plasma observations can at least place lower limits.

First, it is exceedingly unlikely that Jupiter's outer magnetosphere rotates rigidly and wobbles up and down coincident with the rotational period of Jupiter's tilted magnetic dipole (15° tilt reported by *Smith et al.* [1974*a*]), as suggested by *Van Allen et al.* [1974]. The inferred outer magnetosphere plasma densities are sufficiently high that the measured magnetic field [*Smith et al.*, 1974*a*] would not be able to contain the plasma much beyond about 20 R_J. The complicating factor seems to be the very narrow latitude extent over which energetic charged particles seem to be confined in Jupiter's outer magnetosphere [*Fillius and McIlwain*, 1974; *Simpson et al.*, 1974; *Trainor et al.*, 1974; *Van Allen et al.*, 1974]. A much more plausible model seems to be that suggested by *Smith et al.* [1974*b*], where a disturbance field associated with a current sheet is present in Jupiter's outer magnetosphere. This current sheet lies parallel to Jupiter's equatorial plane, contains the observed quasi-trapped energetic particle population, is the plane of symmetry for the flattened magnetosphere, and moves up and down in latitude coincident with Jupiter's rotational period.

TABLE 3. Measured Average and Calculated Best-Fit Shock Jump Parameters and Sigma Noise Parameters for the Third Shock Crossing Observed by Pioneer 10 for the Outbound Portion of the Jupiter Flyby Trajectory

Parameter*	Average Value	σ	Best-Estimate Value
B_{1x}	0.02	0.30	0.00
B_{1y}	-0.94	0.29	-0.95
B_{1z}	0.27	0.16	0.28
B_{2x}	-2.11	1.06	-1.88
B_{2y}	-1.84	1.02	-1.70
B_{2z}	0.48	0.58	0.46
W_x	55.	20.	78.
W_y	-9.0	20.	0.8
W_z	4.8	15.	1.2
n_1	0.21	0.1	0.18
n_2	0.24	0.15	0.32

*Units of measure are gammas for B_{1x} through B_{2z}; kilometers per second for W_x, W_y, and W_z; and cm^{-3} for n_1 and n_2.

TABLE 4. Estimated Jupiter Magnetospheric Plasma Properties on the Assumption of Pressure Balance Across the Jovian Magnetopause

		Magnetosheath			Magnetosphere		
Date	Time, hours UT	Thermal Pressure, dyn cm^{-2} x 10^{-11}	Magnetic Energy Density, ergs cm^{-3} x 10^{-11}	Calculated Thermal Pressure, dyn cm^{-2} x 10^{-11}	Calculated Beta	Calculated Ion Number Density, cm^{-3}	Magnetic Energy Density, ergs cm^{-3} x 10^{-11}
Dec. 10	1153	12	44	12	0.28	8.4	44
Dec. 13	0158	0.4*	2.9	0.4	0.13 ~0.2†	0.27 0.43†	2.9
Dec. 14	1850	7.1	4.1	7.6	2.1 ~2.8†	5.5 7.3†	3.6

*Measured value that is not too reliable.
†Estimated by using aerodynamic analogy.

The question of the degree of flattening for Jupiter's outer magnetosphere still remains. During the inbound portion of the Pioneer 10 trajectory the magnetopause was first observed at approximately 96 R_J, and the spacecraft remained inside the magnetosphere for several days and, of course, many Jupiter rotational periods. Since the magnetosheath was not observed during this period and since the Pioneer 10 spacecraft was 7 R_J below Jupiter's equatorial plane, it then follows that the thickness of Jupiter's magnetosphere must be at least 4 times this distance, or 28 R_J. Likewise, on the dawn side of Jupiter for the outbound pass the spacecraft was within the magnetosphere for many Jupiter rotational periods prior to the last magnetopause crossing at approximately 150 R_J. In this region, Pioneer 10 was 24 R_J above Jupiter's equatorial plane, thus suggesting that here Jupiter's magnetosphere must be at least 96 R_J thick. These are probably conservative lower limits for the magnetospheric thickness, at least since fluctuations in the polar flow direction of the interplanetary solar wind would require the magnetosphere to be thicker than the above values in order to avoid detection of the magnetosheath for time periods greater than one Jupiter rotation. Perhaps further detailed analysis and correlation of plasma and magnetic field data could be used to increase these lower limits of the magnetospheric thickness.

One further argument against a disklike magnetosphere and in favor of a magnetosphere with reasonable thickness is the second inbound magnetosheath observation made near 50 R_J. If Jupiter's magnetosphere were a disk with the subsolar point near 100 R_J, then it could be argued that a simple shift in the solar wind polar flow direction could deflect the 'magnetodisk' such that the Pioneer 10 spacecraft would enter the magnetosheath. If this were true, the spacecraft would find itself some 50 R_J downstream from the subsolar point, and one would expect the magnetosheath plasma flow to be nearly solar radial. This in fact was not observed, but rather the flow directions observed during the second magnetosheath traversal were incident from large angles with respect to the solar direction and quite similar to those observed during the first magnetosheath crossing. In addition, Jupiter's outer magnetosphere is apparently a high-beta region with inferred thermal plasma densities of the order of a few per cubic centimeter. This finding is supported by the outer magnetosphere magnetic field observations [*Smith et al.*, 1974*a*], where hourly averaged field strengths are only slowly increasing from about 5–6 γ at 100 R_J to slightly over 10 γ at 30 R_J. Thus the entire outer portion of Jupiter's magnetosphere is highly inflated and therefore highly responsive to changes in the dynamic pressure of the solar wind.

A crude calculation shows that for the estimated internal pressure of Jupiter's outer magnetosphere an increase in the solar wind dynamic pressure of only a factor of 3 is all that would be required to contract the magnetosphere from 100 R_J down to less than 50 R_J. At the time of the Pioneer 10 encounter, Pioneer 11 was 2.2 AU upstream from Jupiter and almost aligned along the same solar radial (0.8° angular difference in solar longitude between Pioneer 11 and Jupiter). Approximately 7 days and 17 hours prior to the second inbound magnetosheath traversal by Pioneer 10 a solar wind dynamic pressure increase of approximately 4 was observed by Pioneer 11. The delay time expected for this dynamic pressure increase to reach Jupiter is in excellent agreement with the entry of Pioneer 10 into Jupiter's magnetosheath for the second time during the inbound pass. Inspection of the hourly averaged magnetic field values for this second magnetosheath traversal [*Smith et al.*, 1974*a*] shows a much higher field strength here than for the first traversal, indicating that the magnetosheath field has been compressed. Therefore it is postulated that Jupiter's magnetosphere contracted by at least a factor of 2 in response to an increase in the solar wind dynamic pressure such that the Pioneer 10 spacecraft became imbedded in Jupiter's magnetosheath for the second time during the inbound leg.

The large number of magnetopause and shock crossings observed during the outbound pass further argues for the great responsiveness that Jupiter's outer magnetosphere must have to changing conditions in the solar wind. For this reason and the arguments in favor of a reasonably thick magnetosphere the anomalously short distance observed across the first magnetosheath traversal is considered to be best accounted for by an outward expansion of Jupiter's magnetosphere at that time.

A fundamental remaining question is if Jupiter's magnetosphere has a reasonable thickness, then why is the energetic particle population constrained to such a narrow disk in the outer magnetosphere? Could the current sheet suggested by *Smith et al.* [1974*b*] form a sort of magnetic bottle, or is there perhaps local acceleration [*Simpson et al.*, 1974]? It is clear that deeper analysis as well as observations on future

Jupiter flybys (such as Pioneer 11) and orbiter missions will be required to shed further light on this question.

Acknowledgments. We are deeply indebted to Ed Smith for providing us with detailed magnetic field data prior to publication. These data have been essential for our shock and pressure balance calculations. We would like to express our appreciation and gratitude to the Pioneer Project Office at Ames Research Center for their hard work and excellent performance, which produced the successful Pioneer 10 Jupiter flyby. We also thank the staff of TRW Systems, Redondo Beach, California, the Pioneer 10 spacecraft contractor, for the design and fabrication of the spacecraft, which has operated flawlessly throughout the entire mission. Finally, we would like to acknowledge the Management and Engineering Staff of Time Zero Laboratories, Torrance, California, for the detailed design and construction of the Pioneer 10 plasma analyzer experiment, which not only has operated flawlessly since launch but also has exceeded operational expectations.

REFERENCES

Fillius, R. W., and C. E. McIlwain, Radiation belts of Jupiter, *Science, 183,* 314, 1974.

Hall, C. F., Pioneer 10, *Science,* 183, 301, 1974.

Lepping, R. P., and P. D. Argentiero, Improved shock normals obtained from combined magnetic field and plasma data from a single spacecraft, *NASA-GSFC Rep. X-692-70-276,* July 1970. (Also *J. Geophys. Res., 76,* 4349, 1971.)

Simpson, J. A., D. Hamilton, G. Lentz, R. B. McKibben, A. Mogro-Campero, M. Perkins, K. R. Pyle, A. J. Tuzzolino, and J. J. O'Gallagher, Protons and electrons in Jupiter's magnetic field: Results from the University of Chicago experiment on Pioneer 10, *Science, 183,* 306, 1974.

Smith, E. J., L. Davis, Jr., D. E. Jones, D. S. Colburn, P. J. Coleman, Jr., P. Dyal, and C. P. Sonett, Magnetic field of Jupiter and its interaction with the solar wind, *Science, 183,* 305, 1974*a*.

Smith, E. J., L. Davis, Jr., D. E. Jones, P. J. Coleman, Jr., D. S. Colburn, P. Dyal, C. P. Sonett, and A. M. A. Frandsen, The planetary magnetic field and magnetosphere of Jupiter: Pioneer 10, *J. Geophys. Res., 79,* this issue, 1974*b*.

Spreiter, J. R., A. L. Summers, and A. Y. Alksne, Hydromagnetic flow around the magnetosphere, *Planet. Space Sci., 14,* 223, 1966.

Trainor, J. H., B. J. Teegarden, D. E. Stilwell, F. B. McDonald, E. C. Roelof, and W. R. Webber, Energetic particle population in the Jovian magnetosphere: A preliminary note, *Science, 183,* 311, 1974.

Van Allen, J. A., D. N. Baker, B. A. Randall, M. F. Thomsen, D. D. Sentman, and H. R. Flindt, Energetic electrons in the magnetosphere of Jupiter, *Science, 183,* 309, 1974.

Wolfe, J. H., H. R. Collard, J. D. Mihalov, and D. S. Intriligator, Preliminary Pioneer 10 encounter results from the Ames Research Center plasma analyzer experiment, *Science, 183,* 303, 1974.

(Received May 29, 1974;
accepted June 21, 1974.)